Süleyman Demirel Üniversitesi
Fen Bilimleri Enstitüsü Dergisi
Cilt 21, Sayı 2, 338-344, 2017

Süleyman Demirel University
Journal of Natural and Applied Sciences
Volume 21, Issue 2, 338-344, 2017

DOI: 10.19113/sdufbed.54180

Measurements of Proton Energy Spectra Generated by Ultra Intense Laser Solid Interactions

Özgür CULFA[*1]

[1]Karamanoğlu Mehmetbey Üniversitesi, Kamil Özdağ Fen Fakültesi, Fizik Bölümü, 70100, Karaman

(Alınış / Received: 17.03.2017, Kabul / Accepted: 24.04.2017, Online Yayınlanma / Published Online: 06.06.2017)

Keywords
Proton generation,
Lazer solid interactions,
High power lasers

Abstract: In this study, we have presented proton energy spectra produced by such high irradiance (10^{20} W/cm^2) lasers interacting with a pre formed plasma in front of the target and with solid targets without a pre formed plasma. The effects of the target thickness and the generated plasma on the maximum energy and proton numbers are assessed. It is observed that experimentally measured maximum proton energy and number of protons have a dependence on target thickness and preformed plasma scale length produced by prepulse laser with the irradiance of $\sim 10^{12}$ W/cm^2. 2D EPOCH PIC code simulation results of the energy spectra of protons are in a good agreement with measured experimental results.

Ultra Yoğun Lazer-Katı Etkileşimleri Sonucu Üretilen Proton Enerji Spektrumlarının İncelenmesi

Anahtar Kelimeler
Proton üretimi,
Lazer madde etkileşimleri,
Ultra yoğun lazerler

Özet: Yapılan bu çalışmada,ultra yoğun lazerlerin (10^{20} W/cm^2) farklı kalınlıktaki katı hedeflerle etkileşimi sonucu üretilen protonlar incelenmiştir. Ayrıca ana lazerden önce kullanılan ve younluğu $\sim 10^{12}$ W/cm^2 seviyesinde olan ikincil lazerle önceden oluşturulmuş plazmaların, üretilen protonların enerji spektrumları üzerindeki etkisi araştırılmıştır. Ana lazer tarafından ateşlenen katı hedeflerin kalınlığının, üretilen protonların yoğunluğu ve maksimum enerjilerine olan etkisi, ayrıca katı maddelerin ön kısmında (lazerle etkileşimin gerçekleştiği bölge) ikincil lazer tarafından önceden oluşturulan plazmaların hızlandırılan protonlar üzerindeki etkisi çalışılmıştır. 2 boyutlu EPOCH PIC simülasyonlarının sonuçları deneysel verilerin sonuçları ile karşılaştırılmış ve elde edilen bulguları desteklediği gözlemlenmiştir.

1. Introduction

Recent developments on high power lasers enable to reach irradiances exceeding 10^{21} W /cm^2 helping access to new physics phenomena [1]. These developments also enable to access new applications of laser plasmas previously impossible at lower laser intensities. Ultra-bright pulses of high energy protons,electrons and x-rays are generated by laser plasma interactions [2, 3]. Hot electrons and fast ions generated by ultra intense lasers are able to ignite fusion reactions by compressing D-T fuel which enables the 'fast ignition'approach more feasible [4].

For potential applications of proton beams generated by high irradiance lasers such as proton radiography [7], proton accelerators [5], material structure investigations [6] and fast ignition with proton beams [4], the production of proton beam with tunable parameters like energy spectrum, spatial profile and brightness is very important. In order to investigate the effects of target material and thickness [8–10], as well as effect of preformed plasma scale length on generated proton energy [11–13] systematical studies were carried out.

Laser absorption mechanisms have a dependence on plasma scale length which are generally determined by laser pre-pulses. Gradients of the density profile are hard to drop below the irradiance threshold ($< 10^9$ W /cm^2) for plasma generation due to the essential high laser contrast ($> 10^{11}$) related to the high irradiance. In order to increase the incoming laser contrast, plasma mirrors have been utilised so as to enable high power laser irradiance onto initially unperturbed surfaces of solid targets [14, 15]. As an alternative, the production of fast protons, electrons and x-rays can be increased by deliberately generated preformed plasma scale length [11, 13, 16]. In our previous study, we have investigated the variations of proton temperatures and the number of protons for different density gradients generated by a deliberate pre pulse and target thickness experimentally and therotically [26].

It is well known that laser absorption mechanisms strongly dependent on the plasma density gradients. Resonance absorption mechanism [18] presents an optimal absorption with a range of density scale length, while vacuum heating

*Corresponding Author: ozgurculfa@kmu.edu.tr

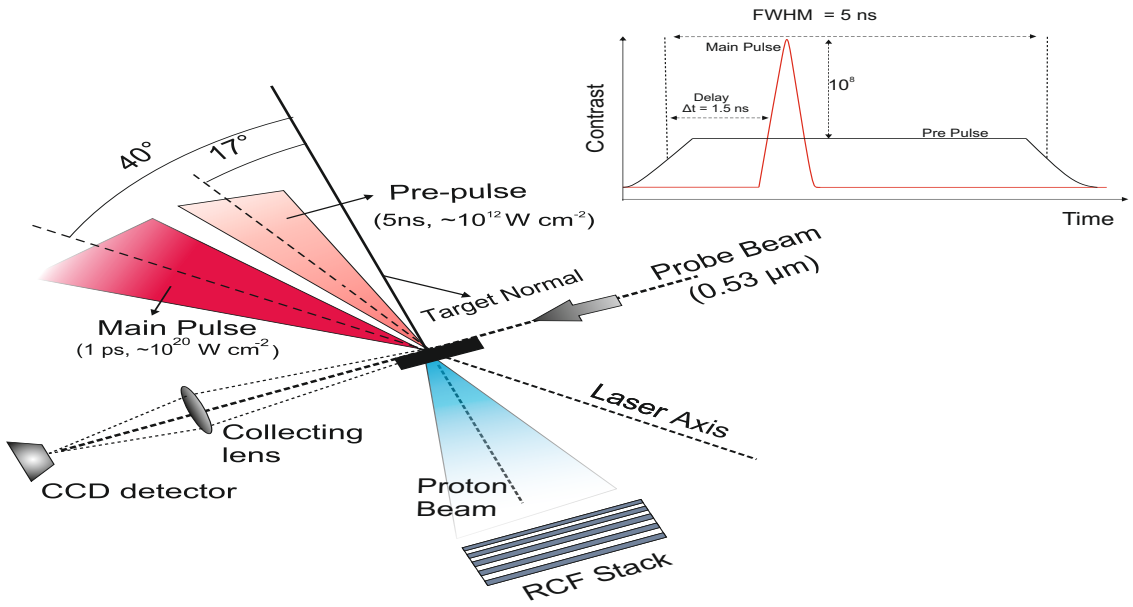

Figure 1. Experimental layout.

[19] terminates when the scale length of the preformed plasma beats the electromagnetic field skin depth. For the longer underdense pulse propagation, the $\mathbf{J} \times \mathbf{B}$ mechanism of electron acceleration in the field of laser is increased. Self focusing enables the modification of laser pulse propagation in longer scale lengths [20] and other effects, including ion channel formation [21] which impacts the energy coupling to electrons. Target Normal Sheath Acceleration (TNSA) is on the process for the laser irradiances of exceeding 10^{18} W /cm^2 by interacting with such thin solid targets. The ultra intense laser pulse interactions with the preformed plasma in front of the solid target forms a source of fast electrons with an energy spectrum relevant to intensity of laser. This generated fast electrons at the front surface of the target enable to get through the target. But the targets capacitance only allows a small amount of the hot electrons to escape before the target is sufficiently charged that leaving the target is almost impossible even for such energetic (MeV) electrons. The remaining hot electrons are confined to the target and bounce back and forward through the target which expands and forms a charge separation field on both sides over a Debye length. Because of the short time scales involved and the induced electric fields are of the order of several TV/m, there is no screening plasma at the rear side of the target. Such fields are able to ionise and accelerates ions through the initially unperturbed surface.

Experimental parameter studies showing the effects of target thickness and the plasma scale-length at the front of the target are useful in elucidating understanding and in the development of applications of laser-accelerated protons arising from the rear side of the target. We present measurements of the maximum energies of protons accelerated from the rear of targets along the target normal in ultra-intense irradiation at 10^{20} W cm^{-2}. We have deliberately used a pre-pulse to irradiate the target before the high power laser irradiation in order to establish a plasma of controlled scale-length into which the high power laser interacts. The scale-length of the plasma formed by the pre-pulse at the time of the high power laser irradiance is measured using transverse probe shadowgraphy. Electron energy and temperature measurements with the controlled density scale-length have been reported by [17, 22]. Experimentally measured proton temperature and number of generated protons have also been studied depending on measured plasma scale length and target thickness previously [26]. This reported study investigates the effects of the target thickness and plasma scale length on measured maximum energy of accelerated protons and the number of protons generated by ultra power lasers through the target normal at the back of the target. we present ion energy spectra, measured maximum ion energies and number of protons depending the plasma density scale-length and target thickness. Our experimental measurements are in agreement with 2D particle-in-cell (PIC) code simulations.

2. Material and Method

2.1. Experimental Setup

Rutherford Appleton Laboratory (RAL) gives the opportunity to access the Vulcan laser system which has been used for the measurement of proton energies. The petawatt (PW) laser has the wavelength of 1.054 micron laser pulses with $\sim$ 1 picosecond pulse duration and energies 150 ± 20 Joule with an intensity contrast of 10^8. Laser irradiance of 10^{20} W/ cm^2 in a p polarized beam was with an incidence angle of 40° to direction of target normal.

A pre-pulse with a pulse duration of 5 ns with an incidence angle of 17° with peak irradiance 1.5 ns before the main pulse. The PW laser was focused onto target of parylene-N (CH) in various thicknesses from 6 to 150 μm. The experiment layout is schematically presented in Figure 1.

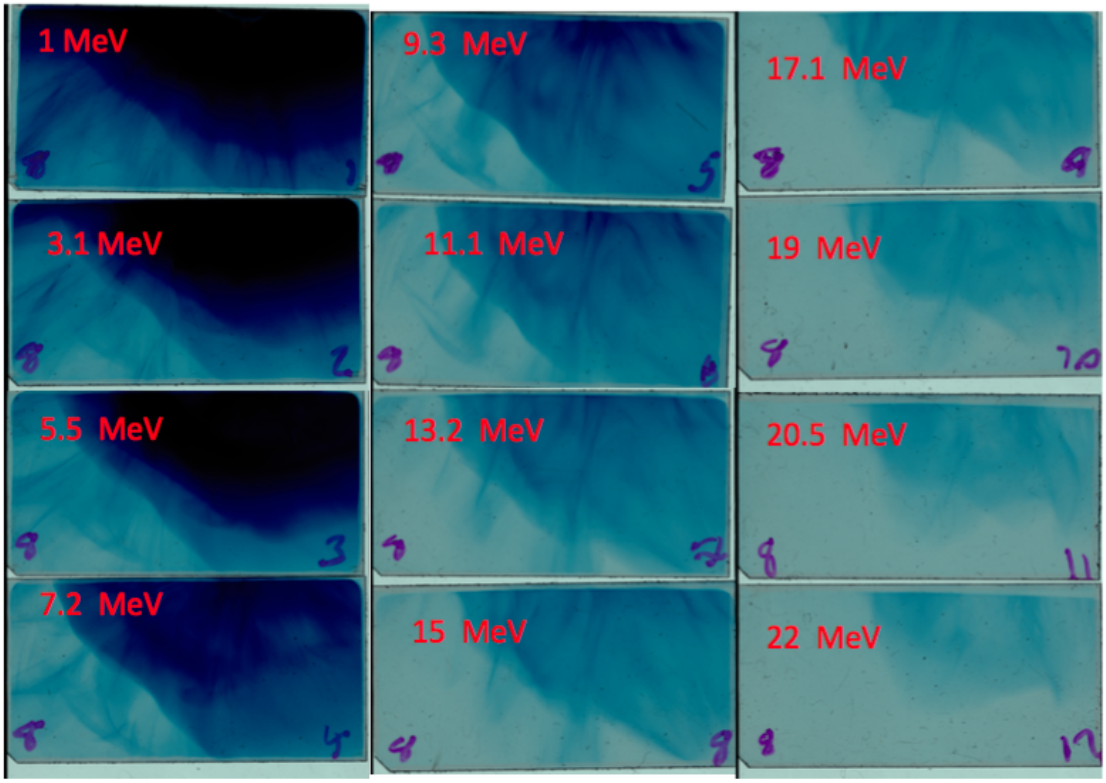

Figure 2. Sequence of RCF films exposed to a proton beam driven by VULCAN Petawatt Laser Facility. The numbers,on each layer marked with red label on the top left corner, correspond to the respective endpoint energies and represent the deposited dose mainly caused by the prominent energy deposition at the end of the particle range (Bragg Peak). Experimental data obtained from 0.1 μm Al buried by 5 μm CH on the front and 105 μm CH on the rear side, irradiated with laser intensity of 2.5×10^{20} W/ cm^2 without prepulse.

A 2ω probe beam was produced from the main beam and used to record the preformed plasma profile at the time of the interaction pulse. The probe beam was transverse to the target surface passing through the plasma generated by the pre pulse laser target interaction. In previous studies [22], we have discussed in detail how to measure and analyse plasma scale length from the shadowgraphy images obtained using the optical probe.

The distrubiton of multi-MeV protons along the target normal from the rear of the target were measured depending on energy using passive stacks of dosimetry radiochromic film (RCF)[23], which were located 5 cm from the back of the target and centered on the target normal direction. Number and energy of accelerated protons were measured as a function of target thickness and the plasma scale length which varies with the pre-pulse intensity[17].

3. Results

3.1. Experimental Results

The radiograph was saved using a radiochromic film stack (Gafchromic HD-810) with a 10 μm thick aluminum foil in front of the stack as a filter to prevent unwanted laser light and expected plasma thermal emission from the rear of the target. The high intensity short pulse laser irradiated a 100 μm CH foil (mentioned above), and by the target normal sheath acceleration mechanism, a proton beam with a cutoff energy around 30 MeV was generated.

The produced hot electron flux with the energies up to 200 MeV is accelerated through to the laser axis (40 $^\circ$ to the target normal and RCF stack) [22]. Protons are attenuated in the stack of RCF films as they penetrate through the different films, with the exposure of the films giving the energy of proton flux sufficient to transmit through the RCF films.

Figure 2 shows an example of RCF outputs taken during the experiment for 0.1 μm Al buried by 5 μm CH on the front and 105 μm CH on the rear side, irradiated with laser intensity of 2.5×10^{20} W/ cm^2 without prepulse. Each RC film layer corresponds to a dose distribution at a certain depth in the RCF material and the Bragg peak energy of protons stopping in the according layer. Deposited energy of protons on each layer of RC films are shown on Figure 2. Deposited dose on films are proportional to the darkness on images which means that more protons are detected on the first RC film and less number of protons are observed with increasing energy.

Each film exposures predominantly at a specific proton energy due to the Bragg peak. The background RCF film exposures includes expose due to hard x-ray emission and is subtracted from exposure measurements. Details of the RCF measurements and the method of analysis of proton energies is given by Schollmeier et al[24].
Proton numbers recorded from the back of the target were found to peak on the target normal axis consistent with TNSA acceleration. In order to compare maximum proton

energy and number of protons obtained from CH foils as a function of plasma scale length and target thickness, we have used a deliberate prepulse in our experiment to vary plasma scale length and different target thicknesses between 10 μm and 140 μm. For each shot, we could identify a proton beam along target normal direction on the RCF stack that is produced independently of the target thickness.

Experimentally measured maximum proton energy as a function of the measured plasma scale length has been shown at Figure 3. It is seen that measured maximum energies increase up to a certain point and start decreases again which is in agreement with previous studies undertaken by Ross et al. [13]. We have explained measured hot electron spectra and showed the decrease on hot electron temperature which is relevant to the plasma scale length and laser filamentation in plasmas [17, 22]. These laser filamentations are also effect generated proton energy and temperature which explains the decrease on proton energy and temperature after a certain scale length.
Generated proton maximum energy was investigated previously. According to the scaling law given by Beg et al [25] (equation 1), the maximum energy of generated protons are around 30 MeV which proves our experimental measurements on maximum proton energy.

$$E_{max} = 1.2 \pm (0.3) \times 10^{-2} [I/(\mathrm{W/cm^2})]^{0.313 \pm 0.03} \quad \mathrm{keV} \tag{1}$$

[25]

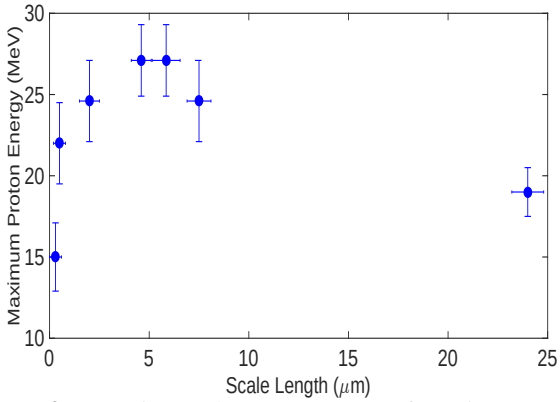

Figure 3. Experimental measurements of maximum proton energy versus generated plasma scale length for individual laser shots

The number of fast electrons increases with the density scale length [17] and this results in a larger number of protons with increasing scale length [26]. Proton generation in a laser-produced plasma is relevant to fast electrons which set up TNSA sheath at the back of the target. Due to high-energy electrons driven by the laser on the target surface, the well known effect responsible for the ion acceleration is charge separation [27–29]. Electron bouncing inside the target enhance the sheath acceleration so thicker targets do not allow fast electron circulation as much as thin foils inside the target. Since fast ions are accelerated inside the TNSA sheath field, generated ion energies and number of fast ions decreases with increasing target thickness (see Figure 4 and 5).

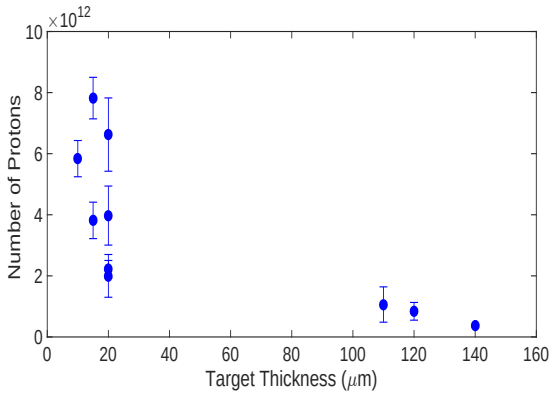

Figure 4. Experimental measurements of number of protons per MeV versus the target thickness for a number of individual laser shots with a front surface scale length of $\sim 1\mu$m.

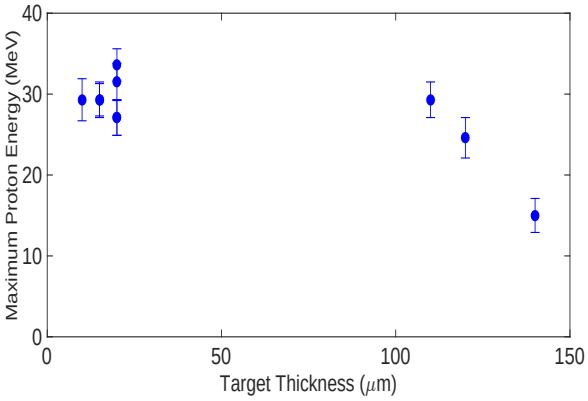

Figure 5. Experimental measurements of maximum proton energy depending on the target thickness for a number of individual laser shots

Figure 4 shows experimental measurements of number of protons per MeV as a function of the target thickness when there is no deliberate prepulse. During the experiment, we have not used any pulse cleaning method such as plasma mirror etc so there were always some preformed plasma however our measurement techniques were not accurate enough to measure that scale length and we are assuming that the plasma scale length generated by the main pulse between 0 and 1 μm. As a result, there are some fluctuations on our measurements for the target thickness. Hownever, general trend is obvious that generated number of protons are higher for thin targets but when the target thickness are increased, we have observed less protons. We know that stopping power of the target is not effective in that thickness for such energetic protons. 2D PIC codes were run to investigate generated number of protons and the TNSA sheath field effect on accelerated protons. Figure 6 shows simulated TNSA sheath field set up by hot electrons, red dashed lines show the TNSA sheath distance. Increasing thicknesses on targets reduce the TNSA sheath field as expected and resulting less number of generated protons.

Figure 5 shows experimental measurements of maximum proton energy when there is no additional prepulse. Ex-

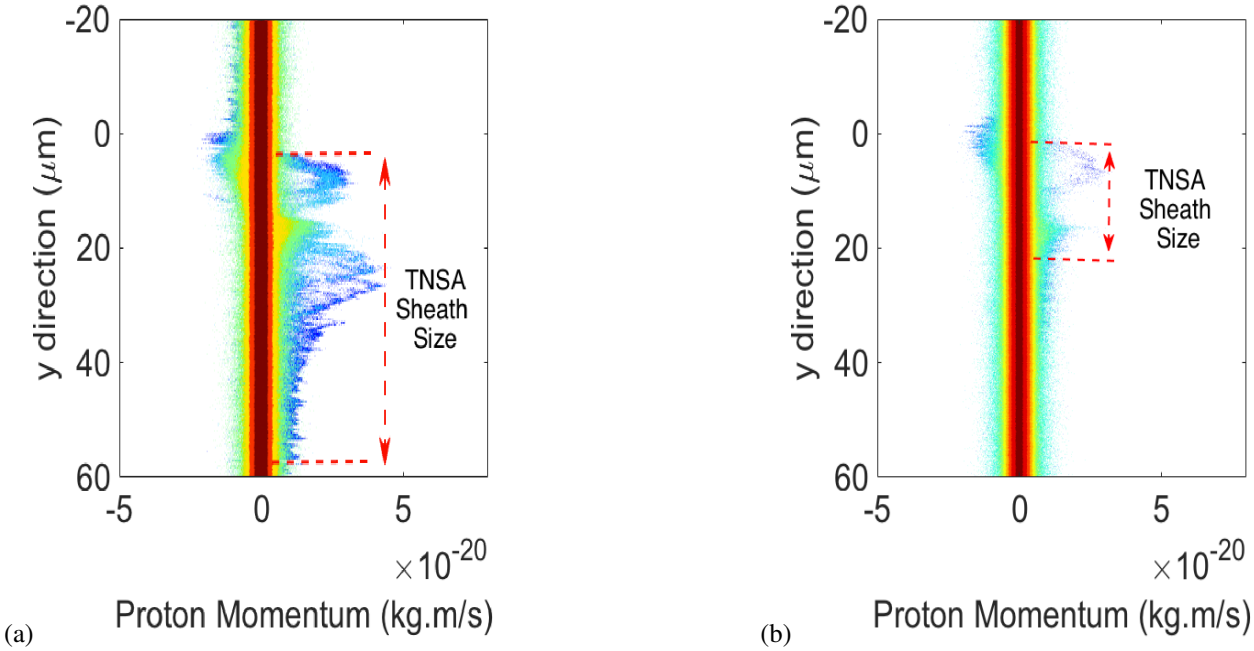

Figure 6. An example of proton phase space profile after 0.55 ps with a) 50 μm , b) 100 μm target thickness as simulated by two dimensional PIC code (EPOCH). The dashed horizontal lines indicates TNSA sheath distance.

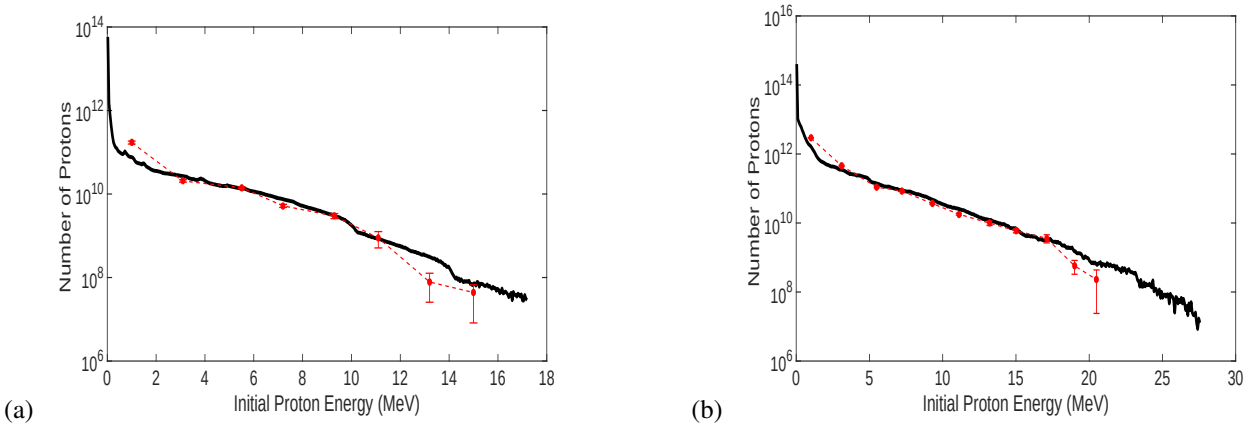

Figure 7. Simulation results compared to experimental proton energy spectra for a) 0.3 μm , b) 7 μm scale length. The continuous black line represents the simulation results, while the red dotted points are the experimental data.

perimentally measured maximum energies of protons are higher for thin targets ($\sim 20\mu$m) but energy of accelerated protons decrease for thicker targets ($\sim 100\mu$m). It is mainly due to the generated sheath field behind the target since the hot electrons can not sufficiently setup sheath electric field on thicker targets. Previous theoretical studies show that maximum energy of generated protons is inversely proportional to the irradiated target thickness which proves our experimental measurements [30].

3.2. Comparison of 2D PIC Code Simulations Results with Experimentally Measured Proton Spectra

In order to understand generated proton behaviour with varying target thickness and plasma scale length, we have run 2D EPOCH PC simulations.

The two dimensional PIC code EPOCH [31] was run to simulate the experimental proton spectra for different target thicknesses and plasma density scale length. The simulation box was 90 μm $\times$ 90 μm defined by 1000 $\times$ 1000 cells with 48 particles which are protons and electrons per cell. The experimental parameters of proton energy spectra for varying target thicknesses with the laser intensity of $3.5 \times 10^{20}\,\mathrm{W/cm^{-2}}$ focussed on a 7 micron focal spot. The incidence angle of 40° was determined. The laser pulse duration and wavelength were 1 ps and 1μm, respectively. The maximum electron density was limited at 50 n_c where n_c is the critical density.

The proton energy spectra was extracted at time 0.5 ps. Figure 7 compares the experimental proton energy spectra to the generated proton spectra from the EPOCH 2D PIC simulation results for different plasma scale length. The red dotted line with circles show our experimental measurements and the continuous line represent the EPOCH 2D PIC code simulation results. Experimentally measured temperature of generated protons have been compared to the simulation results which gives a good agreement [26]. In this work, we are not capable of comparing experimentally detected maximum energies with simulation

results since the number of particles inside the simulation can effect the simulated maximum energies. So we only compared the energy spectra of the experimental and simulation results in the same plot which is in the good agreements for varied plasma scale lengths.

4. Discussion and Conclusion

We have presented measurements of number and energy of protons in high irradiance laser plasma interactions with a preformed plasma of measured density scale length and different target thicknesses when there is no additional pre pulse which generates preplasma before interaction. Previous studies mainly investigated the plasma scale length effect on the backside of the target on proton energies and found that increasing scale length on the back of the target reduces the generated proton energy and they measured proton energies around 20 MeV when there is no plasma scale length at the rear side of the target and for the existence of plasma scale length, the measured proton energy dropped down to 5 MeV with similar target thicknesses and the laser irradiances of $5x10^{19}$ W/cm^2 [11]. Another experimental study also measured around 20 MeV energetic protons for the laser irradiance of $5x10^{19}$ W/cm^2 and 25 μm lead blocks when there is a 10 μm measured scale length [29].
The experimentally observed maximum proton energies increase up to a certain scale length and decrease for longer scale lengths as predicted by a 2D PIC code in our previous work which is mainly because of the laser filamentation inside the plasma.

Generated number and energy of protons decreases with increasing target thickness. Our 2D simulation showed that fast electrons cannot set up a shied field which accelerates protons behind the target so thicker targets are not efficient to use to generate higher proton flux with more energetic protons. Our experimental and simulation parameter studies of proton energies from high irradiance laser plasmas show that the 2D PIC code simulations are accurate and can be useful in the development of applications for laser accelerated protons.

Acknowledgment

The author gratefully acknowledge his colleagues, namely, G.J. Tallents, A.K. Rossall, M.E. Korkmaz, E. Wagenaars, C.P. Ridgers, C.D. Murphy, L.A. Wilson, D.C. Carroll and N.C. Woolsey who really helped during the production of the paper. The author also would like to acknowledge Vulcan Petawatt laser operations, target preparation and engineering staff at the Central Laser Facility of RAL. Research partly was supported by Karamanoglu Mehmetbey University research projects 37-M-16 and 40-M-16 and The Scientific and Technological Research Council of TURKEY (TUBITAK) research project 116F042.

References

[1] Tabak, M., Hammer, J., Glinsky, M. E., Kruer,W. L., Wilks, S. C., Woodworth, J., Campbell, E. M., Perry, M. D. and Mason, R. J. Ignition and high gain with ultra powerful lasers. Phys.Plasmas, 1 (1994),1626-1635.

[2] Daido,H., Nishiuchi, M., and Pirozhkov,A. S. Review of laser-driven ion sources and their applications. Rep.Prog.Phys., 75(2012), 056401.

[3] Macchi, A., Borghesi, M., and Passoni, M. Ion acceleration by superintense laser-plasma interaction. Rev. Mod. Phys., 85 (2013), 751-793.

[4] Roth, M., Cowan, T. E., Key, M. H., Hatchett, S. P., Brown, C., Fountain, W., Johnson, J., Pennington, D. M., Snavely, R. A., Wilks,S. C., Yasuike, K., Ruhl, H., Pegoraro, F., Bulanov, S. V., Campbell, E. M., Perry, M. D. and Powell, H. Fast Ignition by Intense Laser-Accelerated Proton Beams. Phys.Rev.Lett., 86 (2001), 436.

[5] Malka, V., Faure, J., Gauduel, Y. A., Lefebvre, E., Rousse, A., and Phuoc, K. T. Principles and applications of compact laser–plasma accelerators. Nat.Phys., 4(2008) , 447 - 453.

[6] Gemmel, D. S. Channeling and related effects in the motion of charged particles through crystals. Rev.Mod.Phys., 46 (1974),129.

[7] King, N.S.P., Ables, E., Adams, K., Alrick, K.R., Amann, J.F., Balzar, S., et al. An 800-MeV proton radiography facility for dynamic experiments. Nucl. Instrum. Methods Phys. Res.,Sect. A, 424 (1999), 84.

[8] Roth, M., Blazevic, A., Geissel, M., Schlegel, T., Cowan, T. E., Allen, M., Gauthier, J.-C., Audebert, P., Fuchs, J., Meyer ter Vehn, J., Hegelich, M., Karsch, S., and Pukhov,A. Energetic ions generated by laser pulses: A detailed study on target properties. Phys. Rev. ST Accel. Beams, 5 (2002), 061301.

[9] Mackinnon, A. J., Sentoku, Y., Patel, P. K., Price, D. W., Hatchett, S., Key, M. H. Andersen, C., Snavely, R., and Freeman, R. R. Enhancement of Proton Acceleration by Hot-Electron Recirculation in Thin Foils Irradiated by Ultraintense Laser Pulses. Phys. Rev. Lett., 88 (2002), 215006.

[10] Spencer,I., Ledingham, K. W. D., McKenna, P., McCanny, T., Singhal, R. P., Foster, P. S., Neely, D., Langley, A. J., Divall, E. J., Hooker, C. J., Clarke, R. J., Norreys, P. A., Clark, E. L., Krushelnick,K., and Davies,J. R. Experimental study of proton emission from 60-fs, 200-mJ high-repetition-rate tabletop-laser pulses interacting with solid targets. Phys. Rev. E., 67: 046402, 2003.

[11] Mackinnon, A. J., Borghesi, M., Hatchett, S., Key, M. H., Patel, P. K., Campbell, H., Schiavi, A., Snavely, R., Wilks, S. C., and Willi, O. Effect of plasma scale length on multi mev proton production by intense laser pulses. Phys. Rev. Lett., 86 (2001), 1769-1772.

[12] Kaluza, M., Schreiber, J., Santala, M. I. K., Tsakiris, G. D. Eidmann, K., Meyer ter Vehn, J., and Witte, K. J. Influence of the Laser Prepulse on Proton Acceleration in Thin-Foil Experiments. Phys.Rev.Lett., 93(2004),045003.

[13] Gray, R. J., Carroll, D. C., Yuan, X. H., Brenner,C. M., Burza, M., Coury, M., Lancaster, K. L., Lin, X. X., Li, Y. T., Neely, D., Quinn, M. N., Tresca, O., Wahlstrom, C. G., and McKenna, P. Laser pulse propagation and enhanced energy coupling to fast electrons in dense plasma gradients., New Journal of Physics, 16 (2014),113075.

[14] Dromey, B., Kar, S., Zeph, M., Foster, P. The plasma mirror a subpicosecond optical switch for ultrahigh power lasers. Rev. Sci. Ins., 75(2004), 645-649.

[15] Neely, D., Foster, P., Robinson, A., Lindau, F., Lundh,O., Persson,A., Wahlström, C., and McKenna, P. Enhanced proton beams from ultrathin targets driven by high contrast laser pulses. Applied Physics Letters, 89 (2006), 021502.

[16] Levy, A., Nuter,R., Ceccotti, T., Combis, P., Drouin, M., Gremillet, L., Monot, P., Popescu, H., Reaul, F., Lefebvre, E., and Martin, P. Effect of a nanometer scale plasma on laser-accelerated ion beams. New Journal of Physics, 11 (2009), 093036.

[17] Culfa, O., Tallents, G. J., Wagenaars, E., Ridgers, C. P., Dance, R. J., Rossall, A. K., Gray, R. J., McKenna, P., Brown, C. D. R., James, S. F., Hoarty, D. J., Booth, N., Robinson, A. P. L., Lancaster, K. L., Pikuz, S. A., Faenov, A. Y., Kampfer, T., Schulze, K. S., Uschmann, I., and Woolsey, N. C. Hot electron production in laser solid interactions with a controlled pre-pulse. Phys.Plasmas, 21 (2014), 043106.

[18] Kruer, W. L., 1988 The physics of laser plasma interactions. California, Addison - Wesley Publishing Company.

[19] Brunel, F. Not-so-resonant, resonant absorption. Phys. Rev. Lett., 59 (1987), 52-55.

[20] Max, C., Arons, J., and Langdon, A. B. Self-modulation and self-focusing of electromagnetic waves in plasmas. Phys.Rev.Lett, 33 (1974), 209.

[21] Najmudin, Z., Krushelnick, K., Tatarakis, M., Clark, E. L., Danson, C. N., Malka, V., Neely, D., Santala, M.I.K. and Dangor, A. E. The effect of high intensity laser propagation instabilities on channel formation in underdense plasmas. Physics of Plasmas, 10(2003),438.

[22] Culfa, O., Tallents, G. J., Rossall, A. K., Wagenaars, E., Ridgers, C. P., Murphy, C., Dance, R. J., Gray, R. J., McKenna, P., Brown, C. D. R., James, S. F., Hoarty, D. J., Booth, N., Robinson, A. P. L., Lancaster, K. L., Pikuz, S. A., Faenov, A. Y., Kampfer, T., Schulze, K. S., Uschmann, I., and Woolsey, N. C. Plasma scale-length effects on electron energy spectra in high-irradiance laser plasmas.Phys.Rev.E, 93 (2016), 043201 .

[23] Nurnberg, F., Schollmeier, M., Brambrink, E., Blazevic, A., Carroll, D. C., Flippo, K., Gautier, D. C., Geibel, M., Harres, K., Hegelich, B. M., Lundh, O., Markey, K., McKenna, P., Neely, D., Schreiber, J., and Roth, M. Radiochromic film imaging spectroscopy of laser-accelerated proton beams.Rev.Sci.Inst., 80(2009), 033301.

[24] Schollmeier, M., Geissel, M., Sefkow, A. B. and Flippo, K. A. Improved spectral data unfolding for radiochromic film imaging spectroscopy of laser-accelerated proton beams..Rev.Sci.Inst., 85 (2014), 043305.

[25] Beg, F. N., Bell, A. R., Dangor, A. E., Danson, C. N., Fews, A. P., Glinsky, M. E., Hammel, B. A., Lee, P., Norreys, P. A. and Tatarakis, M. A study of picosecond laser solid interactions. Phys. Plasmas., 4(1997), 447-457.

[26] Culfa, O., Tallents, G. J., Korkmaz, M. E., Rossall, A. K., Wagenaars, E., Ridgers, C. P., Murphy, C. D., Booth, N., Carroll, D. C., Wilson, L. A., Lancaster, K. L. and Woolsey, N. C. Plasma scale length effects on protons generated in ultra-intense laser–plasmas. Laser and Particle Beams, 35(2017), 58-63.

[27] Maksimchuk, A., Gu, S., Flippo, K., Umstadter, D. and Bychenkov, V. Yu. Forward Ion Acceleration in Thin Films Driven by a High-Intensity Laser. Phys. Rev. Lett., 84(2000),4108-4111.

[28] Hatchett, S., Brown, C. G., Cowan, T. E., Henry, E. A., Johnson, J. S., Key, M. H., Koch, J. A., Langdon, A. B., Lasinski, B. F., Lee, R. W., Mackinnon, A. J., Pennington, D. M., Perry, M. D., Phillips, T. W., Roth, M., Sangster, T. C., Singh, M. K., Snavely, R. A., Stoyer, M. A., Wilks, S. C. and Yasuike, K. Electron, photon, and ion beams from the relativistic interaction of Petawatt laser pulses with solid targets. Physics of Plasmas, 7(2000), 2076-2082.

[29] Clark, E. L., Krushelnick, K., Davies, J. R., Zepf, M. Tatarakis, M., Beg, F. N., Machacek, A., Norreys, P. A., Santala, M. I. K, Watts, I., and Dangor, A. E. Measurements of Energetic Proton Transport through Magnetized Plasma from Intense Laser Interactions with Solids. Phys.Rev.Lett., 84(2000), 670-673.

[30] Sentoku, Y., Cowan, T. E, Kemp, A., Ruhl, H. High energy proton acceleration in interaction of short laser pulse with dense plasma target. Phys. Plasmas, 10 (2003), 2009-2015.

[31] Arber, T. D, Bennett, K., Brady, C. S., Lawrence-Douglas, A., Ramsay, M. G., Sircombe, N. J., Gillies, P., Evans, R. G., Schmitz, H., Bell, A. R., and Ridgers, C. P. Contemporary particle-in-cell approach to laser-plasma modelling. Plasma Physics and Controlled Fusion, 57(2015),1-26.